Inorganic Chemistry
Cite This: Inorg. Chem. XXXX, XXX, XXX−XXX
Forum Article
pubs.acs.org/IC

Radical Relatives: Facile Oxidation of Hetero-Diarylmethene Anions to Neutral Radicals

Massimiliano Curcio,[†] Daniel Henschel,[†,‡] Mareike Hüttenschmidt,[†,#] Stephen Sproules,[§] and Jason B. Love*[,†]

[†]EaStCHEM School of Chemistry, University of Edinburgh, The King's Buildings, David Brewster Road, Edinburgh EH9 3FJ, U.K.
[‡]Fakultät für Chemie, Technische Universität München, Lichtenbergstraße 4, 85748 Garching, Germany
[#]Institut für Chemie, Universität Rostock, Albert-Einstein-Straße 3a, 18059 Rostock, Germany
[§]WestCHEM School of Chemistry, University of Glasgow, University Avenue, Glasgow G12 8QQ, U.K.

Supporting Information

ABSTRACT: Furan and thiophene diarylmethenes are potential redox-active ligands for metal centers that could be exploited in the development of nontraditional, stoichiometric, and catalytic redox reactions. As such, we describe here the selective *meso*-deprotonations of dithiophene, difuran, and diimine−difuran diarylmethanes to form the π-conjugated anions, for which only the diimino−difuryl anion is truly isolable and studied by X-ray crystallography. In all cases, facile one-electron oxidation of these anions occurs, which allows the isolation of the neutral dithienyl and diimino−difuryl radicals. UV−Visible and time-dependent density functional theory studies reveal that the oxidation of the dithienyl anion to its radical is associated with an increase in the highest (singly) occupied molecular orbital−lowest unoccupied molecular orbital gap, evident through a hypsochromic shift of the main absorption band in the electronic spectrum, whereas oxidation of the diimino−difuryl anion causes only minor spectroscopic changes. Electrochemical studies support the stability of the radicals with respect to the anion, showing strongly negative oxidation potentials. The control of the redox activity of these diarylmethene carbanions through variation of the nature of the substituents, donor-atom, and the conjugated π-system and their potential as ligands for redox-inert metal centers makes them intriguing candidates as noninnocent partners for redox reactions.

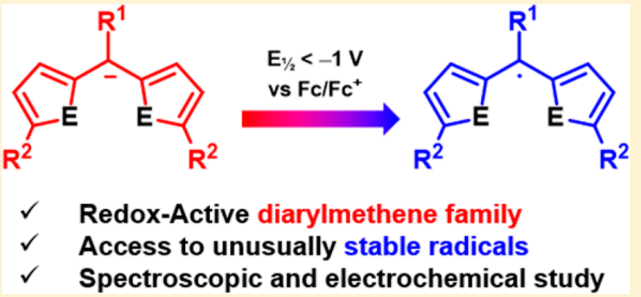

INTRODUCTION

In conventional redox reactions, the redox process is managed solely by a metal center that varies its formal oxidation state according to gain or loss of electrons. In contrast, an increasingly prevalent approach to redox catalysis is to use the redox ability of ligands to store or supply reducing equivalents, so limiting, or negating very high or low metal oxidation states.[1−8] This latter approach takes inspiration from biological systems such as enzymes that use, for example, porphyrin or cubane ligands to store or supply electrons for redox reactions.[9−13] Many metal complexes of redox-active ligands have been developed and studied and display redox chemistry that makes use of both ligand redox activity and the Lewis acidity of the metal center to ensure substrate binding. Important recent advances in this field include the reduction of carbon dioxide at an iron-porphyrin center that occurs only upon double reduction of the porphyrin to a tetra-anion[11,14,15] or the conferment of noble reactivity to non-noble metals such as iron through cooperation with a redox-active pyridinediimine (PDI) ligand.[16]

Diarylmethanes have a rich radical chemistry, with early work showing that radical formation was inherent in the C−C coupling of diarylmethanes to form tetraarylethanes.[17] Neutral diarylmethene radicals have been generated by flash photolysis of diarylmethanes through an oxidation/deprotonation mechanism,[18] and related diarylmethane radical anions have been studied by electron paramagnetic resonance (EPR) spectroscopy.[19,20] Importantly, unlike simple diarylmethanes, the heteroatom congeners such as dipyrrins and dipyridyl-, difuryl-, and dithienylmethenes could potentially act as redox-active chelating ligands to transition metals, having some similarity to the well-exploited β-diketiminate ligand family, which has also been shown to exhibit ligand noninnocence.[21−23] Simple neutral difurylmethene radicals are accessible and have been studied by EPR spectroscopy,[24] and dipyridylmethene complexes of the p-block elements form ligand-radical complexes of varying stability.[25−27] Because of their relevance to porphyrins and the fluorescent properties of boron-dipyrromethene (BODIPY) dyes and related complexes,[28]

Special Issue: Applications of Metal Complexes with Ligand-Centered Radicals

Received: March 2, 2018

Downloaded via KAOHSIUNG MEDICAL UNIV on July 4, 2018 at 07:47:07 (UTC).
See https://pubs.acs.org/sharingguidelines for options on how to legitimately share published articles.

© XXXX American Chemical Society

DOI: 10.1021/acs.inorgchem.8b00554
Inorg. Chem. XXXX, XXX, XXX−XXX

dipyrrins have been extensively studied and shown to exhibit redox activity in their complexes and dipyrrin-fullerene triads.[29−35] Similarly to these studies, we have shown that a simply prepared anionic, imine-expanded dipyrrin acts as a ligand for iron and uranium complexes,[36] the latter showing ligand redox activity.[37] Because of the ligand-based lowest unoccupied molecular orbital (LUMO), the sequential outer-sphere, one-electron reduction of the uranyl(VI) center to U(V) and U(IV) occurs by initial ligand reduction followed by electron transfer to the metal. We also reported the redox-active bis(iminothienyl)methene anion $\mathbf{L}^{\mathbf{NS}-}$ (Figure 1) that

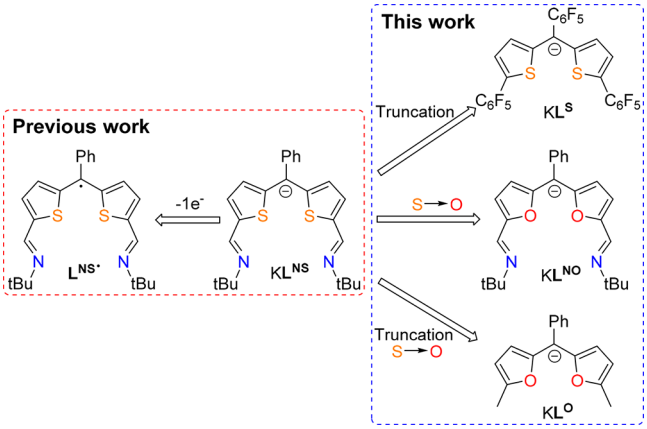

Figure 1. Heterodiarylmethene anions investigated in this work and their relationships to the previously reported imine-expanded dithienylmethene compounds $\mathbf{L}^{\mathbf{NS}}$.

undergoes facile single-electron oxidation to form the stable and isolable neutral iminothiophene radical $\mathbf{L}^{\mathbf{NS}\cdot}$. This radical formed the dinuclear Cu(I) ligand-radical complex $\{CuI\}_2(\mathbf{L}^{\mathbf{NS}\cdot})$ upon reaction with CuI, and under more oxidizing conditions, the radical dication $\mathbf{L}^{\mathbf{NS2}+\cdot}$ was generated.[38] The mild potentials at which these redox processes take place and the poor coordinating ability of the sulfur donors of the thiophene heterocycles prompted us to study additional variants of the diarylmethene scaffold. As such, we describe here the influence of structural variations such as the truncation of the imine functionalities or the use of a stronger coordinating furan heterocycle on the redox and coordination properties of the heterotriarylmethene unit.

EXPERIMENTAL SECTION

General Experimental Details. The syntheses of all air- and moisture-sensitive compounds were performed using standard Schlenk techniques. Vacuum Atmospheres and MBraun glove boxes were used to manipulate and store air- and moisture-sensitive compounds under an atmosphere of dried and deoxygenated dinitrogen. All glassware was dried in an oven at 160 °C, cooled under 1 × 10^{-3} mbar vacuum, and then purged with nitrogen. All solvents for use with air- and moisture-sensitive compounds were stored in ampules containing predried 4 Å molecular sieves. Solvents were collected from a Vacuum Atmospheres solvent tower drying system, where they had been passed over a column of molecular sieves for 24 h prior to collection. They were then degassed prior to use and subsequent storage.

^{1}H NMR spectra were recorded on a Bruker AVA400 spectrometer operating at 399.90 MHz, a Bruker AVA500 or Bruker PRO500 operating at 500.12 MHz, or a Bruker AVA600 spectrometer operating at 599.81 MHz. ^{13}C{^{1}H} NMR spectra were recorded on a Bruker AVA500 or Bruker PRO500 operating at 125.76 MHz. ^{1}H and ^{13}C{^{1}H} NMR spectra are referenced to residual solvent resonances calibrated against $SiMe_4$. ^{19}F{^{1}H} NMR spectra were recorded on a Bruker AVA500 spectrometer operating at 470.59 MHz and referenced to CCl_3F. EPR spectra were recorded on a Bruker ELEXSYS E500 spectrometer, and spectral simulations were performed using Bruker's Xsophe software package. UV−Vis absorption spectra were recorded on a Jasco V-670 spectrophotometer in a 10 mm quartz cuvette fitted with a Young's tap for air-sensitive compounds.

Electrochemical measurements were made using an Autolab ECO Chemie PGSTAT potentiostat, and the data were processed using GPES Manager, version 4.9. Experiments were performed under a flow of N_2 in a 10 mL cell. The solution employed was 1 mM of the analyte in tetrahydrofuran (THF), with 0.1 M [^{n}Bu$_4$N][PF$_6$] as the supporting electrolyte. Cyclic voltammograms were recorded for quiescent solutions at variable scan rates between 100−500 mV s^{-1}. The nature of an observed redox process (reduction or oxidation) was determined by linear sweep voltammetry measured for stirred solutions with scan rates between 10 and 20 mV s^{-1}. The working electrode used was glassy carbon or platinum disc (d = 1 mm) with a platinum gauze counter electrode. Ag^+/Ag pseudoreference electrode was used with potentials calibrated internally against the ferrocenium/ferrocene couple, $Fc^{+/0}$.

X-ray crystallographic data were collected at 170 K on an Oxford Diffraction Excalibur diffractometer using graphite monochromated Mo Kα radiation equipped with an Eos CCD detector (λ = 0.710 73 Å). Structures were solved using ShelXT by direct methods or intrinsic phasing and refined using a full-matrix least-squares refinement on $|F|^2$ using ShelXL.[39,40] All programs were used within the Olex suite.[41] All non-hydrogen atoms were refined with anisotropic displacement parameters, and H atom parameters were constrained to parent atoms and refined using a riding model unless otherwise stated.

Density functional theory (DFT) calculations were performed using the Gaussian09[42] package on the Eddie server system at the University of Edinburgh. Initial guess geometries were generated using the Avogadro program (version 1.1.1). All structures discussed in the text were optimized and converged according to the criteria for maximum displacement and maximum force. Frequency calculations were conducted to confirm that the optimized structures represented minimum energy geometries, which were confirmed by having no imaginary frequencies. The "\OPT = NoRaman" and "\FREQ = NoRaman" options were used to improve computational efficiency. Time-dependent (TD) DFT calculations were conducted on the first 40 excited states using the self-consistent reaction field (SCRF) solvent model (\Solvent = Dichloromethane). All optimization, frequency, and TD-DFT calculations were performed using the CAM-B3LYP functional and 6-311G(d,p) basis set. Molecular orbital surfaces were exported as cubefiles, visualized in UCSF-Chimera,[43] and rendered with the Pov-Ray raytracer program.

Elemental analyses were performed by Mr. Stephen Boyer at the London Metropolitan University and were measured in duplicate.

The reagents 2-bromothiophene, furan, benzaldehyde, $POCl_3$, Amberlyst 15, dimethylformamide (DMF), *tert*-butylamine, and CuI were all used as supplied by Sigma-Aldrich, Fisher Scientific, or VWR. Compounds **1**, **2**, and $H\mathbf{L}^{\mathbf{O}}$ were synthesized according to published procedures.[44−46]

Synthetic Details. *HL*^{S}. A reported procedure was adapted.[11] Solid pentafluorobenzaldehyde (0.925 g, 4.70 mmol), pentafluorophenyl thiophene **1** (3.54 g, 14.1 mmol), and Fe(acac)$_3$ (0.332 g, 0.94 mmol; acac = acetylacetonate) were dissolved in Me_3SiCl (5 mL), purged with argon and stirred at 40 °C for 18 h. The resulting mixture was diluted with CH_2Cl_2, quenched with aqueous $NaHCO_3$, and washed with water and brine before being dried over $MgSO_4$. Evaporation of the solvent provided a yellow/brown solid, which was washed with hexanes to provide the product as an off-white powder (4.09 g, 87%). ^{1}H NMR (500 MHz, chloroform-d): δ = 7.42 (d, J = 3.8 Hz, 2H, γ-C*H*), 7.08 (d, J = 3.8 Hz, 2H, β-C*H*), 6.29 (s, 1H, *meso*-C*H*). ^{13}C{^{1}H} NMR (126 MHz, chloroform-d): δ = 145.1 (m, 2 × C), 145.0 (dm, J = 126 Hz), 143.1 (dm, J = 126 Hz), 141.3 (dm, J = 126 Hz), 140.2 (dm, J = 126 Hz), 138.2 (dm, J = 126 Hz), 130.3 (t, J

DOI: 10.1021/acs.inorgchem.8b00554
Inorg. Chem. XXXX, XXX, XXX−XXX

Scheme 1. Synthesis of the Anionic Hetero-Diarylmethenes KL^S, KL^{NO}, and KL^O and Their Oxidation Reactions[a] to the Corresponding Radicals $L^{S\cdot}$, $L^{NO\cdot}(KI)_n$, and $L^{O\cdot}(KI)_n$

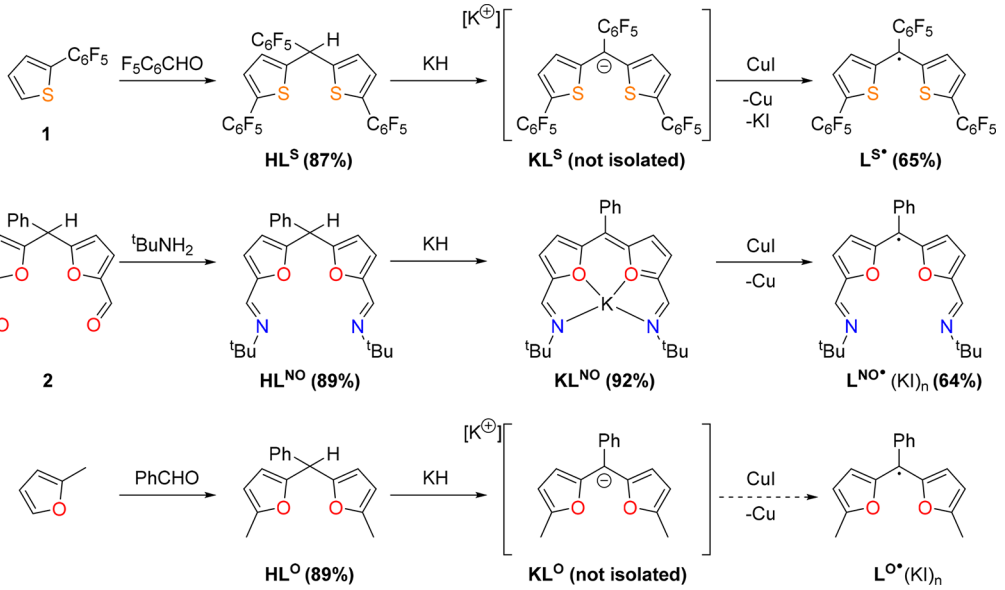

[a]Isolated yields are reported in brackets.

= 5.0 Hz), 127.2 (s), 126.7 (m), 116.1 (t, J = 13.9 Hz), 109.7 (td, J = 15.1 Hz, J = 3.8 Hz), 36.70 (s). ^{19}F NMR (471 MHz, benzene-d_6) δ = −140.5 (d, J = 15.5 Hz), −140.7 (m), −153.4 (t, J = 21.6 Hz), −155.7 (t, J = 21.6 Hz), −160.6 (m), −162.2 (td, J = 21.5, 5.9 Hz). Anal. Calcd for $[C_{27}H_5F_{15}S_2]$: C, 47.8; H, 0.74%; found: C, 47.89; H, 0.76%. High-resolution mass spectrometry (HRMS) atmospheric pressure photoionization (APPI) (m/z): Calcd for $[C_{27}H_4S_2F_{15}]$, 676.950 94; found 677.955 55 $[M\text{-}H]^+$.

KL^S. A solution of HL^S in THF (3 mL) (0.678 g, 1.00 mmol) was added to a suspension of KH (0.048 g, 1.20 mmol) in THF (3 mL), and the resulting mixture was heated at 60 °C for 24 h. Attempts to isolate KL^S resulted in its decomposition upon drying; therefore, no isolated yield is reported. ^{1}H NMR (400 MHz, tetrahydrofuran-d_8): δ = 7.31 (d, J = 4.5 Hz, 2H, γ-C*H*), 5.93 (d, J = 4.0 Hz, 2H, β-C*H*). ^{13}C{^{1}H} NMR (126 MHz, tetrahydrofuran-d_8): δ = 151.5 (2 × C), 147.5 (dm, J = 126 Hz), 142.9 (dm, J = 126 Hz), 140.2 (dm, J = 126 Hz), 139.1 (dm, J = 126 Hz), 135.2 (dm, J = 126 Hz), 132.0 (m), 120.3 (t, J = 20.2 Hz), 114.3 (td, J_1 = 15.1 Hz, J_2 = 2.5 Hz), 110.1 (s), 105.9 (s), 77.9 (s). ^{19}F NMR (471 MHz, tetrahydrofuran-d_8): δ = −139.6 (dd, J = 25.8, 8.2 Hz), −146.1 (dt, J = 22.8, 5.5 Hz), −163.3 (t, J = 20.9 Hz), −166.0 (ddd, J = 25.8, 20.9, 8.2 Hz), −167.5 (td, J = 21.7, 5.3 Hz), −172.2 (tt, J = 21.2, 5.4 Hz). UV−Vis (THF): λ_{max} (ε) 464 nm (9500 dm^3 mol^{-1} cm^{-1}), 636 nm (54 400 dm^3 mol^{-1} cm^{-1}).

$L^{S\cdot}$. A solution of HL^S (0.339 g, 0.50 mmol) in THF (3 mL) was added to a suspension of CuI (0.105 g, 0.55 mmol) and KH (0.024 g, 0.60 mmol) in THF (3 mL), and the resulting mixture was heated at 60 °C for 24 h, providing a yellow/brown solution. Filtration, solvent removal, and washing with hexane provided $L^{S\cdot}$ as a light yellow solid (0.220 g, 65%). UV−Vis (THF): λ_{max} (ε) 211 (17 500), 291 (24 700), 456 nm (2300 dm^3 mol^{-1} cm^{-1}). Anal. Calcd for $[C_{27}H_4F_{15}S_2]$ C, 47.87; H, 0.60%; found: C, 48.01; H, 0.65%. HRMS (APPI): Calcd for $[C_{27}H_4S_2F_{15}]$, 676.950 94; found 676.950 84 $[M]^+$.

$(L^{O\cdot})(KI)_n$. A solution of HL^O (1.260 g, 5.00 mmol) in THF (5 mL) was added to a suspension of CuI (1.140 g, 5.00 mmol) and KH (0.401 g, 10.00 mmol) in THF (5 mL), and the resulting mixture was heated at 60 °C for 24 h, providing a dark brown solution. The crude mixture was cooled to −30 °C and filtered while cold. The filtrate was evaporated to dryness under vacuum and washed with hexanes to provide $(L^{O\cdot})(KI)_n$ as a dark brown solid (0.944 g, 75% based on $L^{O\cdot}$). Anal. Calcd for $L^{O\cdot}$ $[C_{17}H_{15}O_2]$ C, 81.25; H, 6.02%; for $(L^{O\cdot})_2(KI)$ $[C_{17}H_{15}O_2KI]$ C, 61.08; H, 4.52%; found: C, 64.32; H, 4.91%. HRMS (APPI) m/z: Calcd for $[C_{17}H_{15}O_2]$, 251.106 66; found 251.107 43 $[M]^+$. Calcd for $[C_{34}H_{30}O_4]$, 502.213 86; found 502.214 33 $[M + H]^+$.

*Bis(5,5′-formyl-2,2′-furan)phenylmethane, **2***. A reported procedure was adapted.[9] Neat $POCl_3$ (10.0 mL, 107 mmol) was added at 0 °C to a solution of **1** (9.6 g, 42.9 mmol) in DMF (100 mL) providing a light brown mixture that was stirred at room temperature for 24 h, during which the color changed to red/purple. The reaction was quenched by the addition to NaOAc(aq) at 0 °C followed by stirring for 1 h at room temperature. The crude product was extracted in CH_2Cl_2 (150 mL), washed sequentially with water (3 × 50 mL), HCl(aq) (3 × 50 mL), and $NaHCO_3$(aq) (3 × 50 mL) and dried over $MgSO_4$ to obtain a dark red oil. Purification by flash chromatography (hexanes/EtOAc 7:3, R_f = 0.4) provided **2** as a light brown oil (4.2 g, 35%). ^{1}H NMR (500 MHz, chloroform-d): δ = 9.59 (s, 2H, C*H*O), 7.40−7.28 (m, 5H, o-C*H*, m-C*H*, p-C*H*), 7.23 (d, J = 3.6, 2H, β-C*H*), 6.40−6.31 (m, 2H, γ-C*H*), 5.66 (s, 1H, *meso*-C*H*). ^{13}C{^{1}H} NMR (126 MHz, chloroform-d): δ = 177.4 (s), 159.1 (s), 152.5 (s), 136.5 (s), 129.0 (s), 128.2 (s), 128.0 (s), 122.4 (s), 111.3 (s), 45.4 (s).

HL^{NO}. Neat *tert*-butylamine (2.82 mL, 37.2 mmol) was added to a solution of **2** (1.88 g, 9.30 mmol) in toluene (60 mL) and 4 Å molecular sieves (3.0 g), and the resulting mixture was stirred for 36 h at room temperature. The resulting mixture was filtered through diatomaceous earth, and the solvent was removed under vacuum, providing a dark brown oil, which was dissolved in hexanes (30 mL) and filtered to remove undissolved impurities. Evaporation of the filtrate under vacuum provided HL^{NO} as a dark brown solid (3.23 g, 90%). ^{1}H NMR (601 MHz, chloroform-d): δ = 8.02 (s, 2H, N = C*H*), 7.33−7.29 (m, 2H, m-C*H*), 7.28−7.24 (m, 1H, p-C*H*), 7.23−7.20 (m, 2H, o-C*H*), 6.72 (d, J = 3.4, 2H, β-C*H*), 6.10−6.05 (m, 2H, γ-C*H*), 5.65 (s, 1H, *meso*-C*H*), 1.26 (s, 18H, CH_3). ^{13}C{^{1}H} NMR (126 MHz, chloroform-d): δ = 156.5 (s), 152.5 (s), 145.3 (s), 138.8 (s), 128.8 (s), 128.6 (s), 127.5 (s), 113.6 (s), 110.4 (s), 57.7 (s), 45.3 (s), 29.8 (s). Anal. Calcd for $[C_{25}H_{30}N_2O_2]$: C, 76.89; H, 7.74; N, 7.17%; found: C, 76.49; H, 7.52; N, 7.05%. UV−Vis (toluene): λ_{max} (ε) 284 nm (22 000 dm^3 mol^{-1} cm^{-1}). HRMS (electrospray ionization (ESI)) (m/z): calcd for $[C_{25}H_{30}N_2O_2]$, 391.2380; found 391.2356 $[M]^+$.

KL^{NO}. A dark brown solution of HL^{NO} (6.50 mmol, 2.5 g) in THF (15 mL) was added to a suspension of KH (7.80 mmol, 312 mg) in THF (15 mL), and the resulting dark green mixture was stirred at room temperature for 2 h and vented every 30 min. The mixture was

DOI: 10.1021/acs.inorgchem.8b00554
Inorg. Chem. XXXX, XXX, XXX−XXX

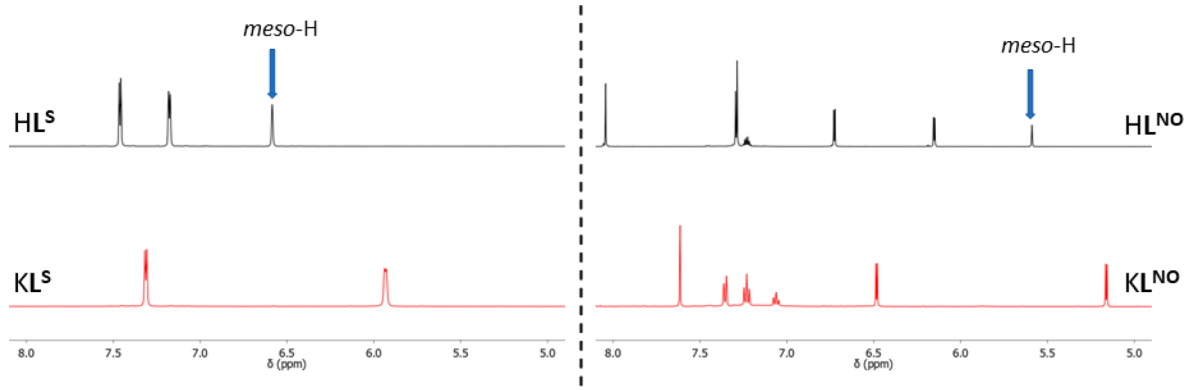

Figure 2. Portion of the ^{1}H NMR spectra (THF-d_8) for HL^S/KL^S (left) and HL^{NO}/KL^{NO} (right).

filtered, and the solvent was evaporated under vacuum to provide KL^{NO} as a brown/gold solid (2.56 g, 92%). ^{1}H NMR (500 MHz, tetrahydrofuran-d_8): δ = 7.61 (s, 2H, N = C*H*), 7.36 (d, J = 7.9, 2H, *o*-C*H*), 7.23 (t, J = 7.5, 2H, *m*-C*H*), 7.09−7.04 (m, 1H, *p*-C*H*), 6.48 (d, J = 4.0, 2H, *β*-C*H*), 5.16 (d, J = 4.0, 2H, *γ*-C*H*), 1.27 (s, 18H, CH_3). ^{13}C{^{1}H} NMR (126 MHz, tetrahydrofuran-d_8): δ = 163.0 (s), 144.3 (s), 143.5 (s), 142.4 (s), 133.6 (s), 128.9 (s), 125.3 (s), 123.8 (s), 96.8 (s), 84.4 (s), 55.7 (s), 31.1 (s). Anal. Calcd for [$C_{25}H_{29}N_2O_2K$]: C, 70.06; H, 6.82; N, 6.54%; found: C, 69.68; H, 6.94; N, 6.42%. UV−Vis (THF): λ_{max} (ε) 269 (28 900), 346 (24 500), 453 (19 400), 630 nm (23 100 dm^3 mol^{-1} cm^{-1}).

($L^{NO\cdot}$)(KI). A dark green mixture of KL^{NO} (1.49 mmol, 640 mg) and CuI (1.47 mmol, 280 mg) in toluene (8 mL) was stirred at room temperature for 72 h, during which it turned dark brown. The mixture was filtered, and the toluene evaporated under vacuum to give a brown solid, which was washed with hexanes (3 × 5 mL) providing ($L^{NO\cdot}$)(KI) as a light brown solid (0.518 g, 64%). HRMS (APPI) (*m*/*z*): calcd for [$C_{25}H_{29}N_2O_2$.], 389.222 35; found 389.221 81 [M]$^+$. Anal. Calcd for $L^{NO\cdot}$ [$C_{25}H_{29}N_2O_2$] C, 77.09; H, 7.50; N, 7.19%; for ($L^{NO\cdot}$)(KI) [$C_{25}H_{29}N_2O_2KI$] C, 54.05; H, 5.26; N, 5.04%; found: C, 57.00; H, 4.93; N, 4.53%.

RESULTS AND DISCUSSION

Synthesis of the Precursors. The synthesis of HL^S involves a two-step procedure starting from 2-bromothiophene with an initial arylation protocol to access the intermediate 2-pentafluorophenylthiophene **1**,[44] followed by an acid-catalyzed condensation with pentafluorobenzaldehyde to provide the desired precursor as an off-white solid (Scheme 1). Similarly, compound HL^O is obtained in a one-step procedure through condensation of benzaldehyde and the commercially available 2-methylfuran **3**;[46] all attempts to prepare pentafluorophenyl-substituted variants of HL^O were unsuccessful. In contrast, the donor-expanded variant HL^{NO} is obtained straightforwardly as a brown/orange solid in high yield through condensation of the dialdehyde intermediate **2**[45] with *tert*-butylamine.

The reactions between HL^S or HL^{NO} and KH both display color changes that are the consequence of the full conjugation of the carbon framework that would be achieved through *meso*-H deprotonation; the thiophene anion KL^S has a dark blue color, whereas the iminofuran anion KL^{NO} displays a dichroic dark green/red color in solution. Further evidence for the *meso*-selective deprotonation is provided in the ^{1}H NMR spectra of these anions, which show the disappearance of the peaks at 6.58 ppm for HL^S and 5.59 ppm for HL^{NO} along with concomitant shifts in the heterocyclic peaks (Figure 2).

Dithiophene HL^S. In the case of HL^S, the choice of pentafluorophenyl as the 5,5′-substituents proved important as alternative alkyl-, aryl-, and fused arene-substituted analogues decomposed upon deprotonation with KH. Even so, while the clean formation of KL^S is seen in the ^{1}H NMR spectrum, it remains highly reactive and slowly decomposes in either THF or pyridine solution to an NMR-silent, dark yellow solution, so precluding its isolation. Additionally, HL^S is sufficiently acidic to be deprotonated by the weaker silylamide base KN(SiMe$_3$)$_2$; however, the resulting blue KL^S solution is gradually oxidized to a paramagnetic species and at a faster rate than seen with KH. As such, a targeted synthesis of the paramagnetic compound was performed by reacting HL^S with KH in the presence of stoichiometric CuI. As the reaction occurs the initial colorless solution turns gradually dark green, then light green, and finally dark yellow as the NMR-silent product $L^{S\cdot}$ is formed. The EPR spectrum of isolated $L^{S\cdot}$ shows a resonance at g_{iso} = 2.0036, consistent with an organic radical (Figure 3). The hyperfine structure is highly complex due to the coupling of the unpaired electron to all four protons from the thienyl moieties and all 15 fluorine atoms (^{19}F, I = 0.5, 100% abundant) of the pentafluorophenyl substituents.

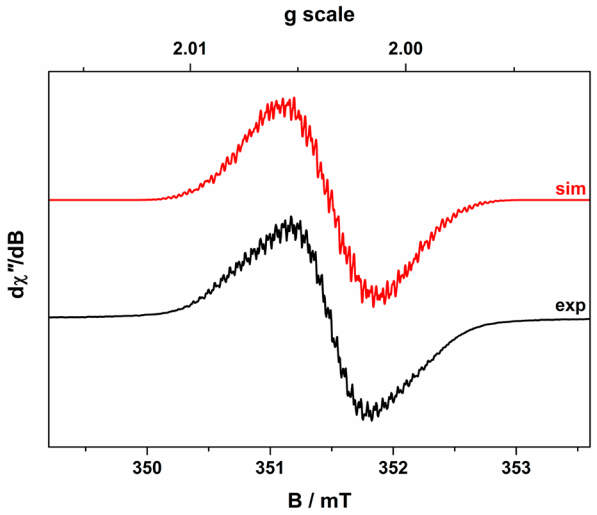

Figure 3. X-band EPR spectrum of radical $L^{S\cdot}$ in CH_2Cl_2 at 293 K (experimental conditions: frequency, 9.8562 GHz; power, 2.0 mW; modulation, 0.01 mT). Experimental data are represented by the black line with the simulation depicted by the red trace. g_{iso} = 2.0036; A_{iso} = 3.71 × 10^{-4} cm^{-1} (2 × ^{1}H); A_{iso} = 3.05 × 10^{-4} cm^{-1} (2 × ^{1}H); A_{iso} = 1.71 × 10^{-4} cm^{-1} (3 × ^{19}F); A_{iso} = 1.16 × 10^{-4} cm^{-1} (6 × ^{19}F); A_{iso} = 0.47 × 10^{-4} cm^{-1} (2 × ^{19}F); A_{iso} = 0.34 × 10^{-4} cm^{-1} (4 × ^{19}F).

DOI: 10.1021/acs.inorgchem.8b00554
Inorg. Chem. XXXX, XXX, XXX−XXX

Interestingly, the dithienyl radical $\mathbf{L}^{S\cdot}$ is a stable acyclic radical that, in contrast to its imine-expanded relative, possesses a less extensive π-system with consequent minimal stabilization by conjugation. In addition, it would be expected that the strongly electron-withdrawing pentafluorophenyl substituents would destabilize the radical in favor of the anion. Because of the redox activity displayed by this simple dithienyl compound, reactions between $\mathbf{KL}^{S}$ and a variety of metal salts were attempted to access metal complexes of this potentially redox-active ligand. Unfortunately, these reactions result in ligand oxidation to form $\mathbf{L}^{S\cdot}$, even in the case of typically redox-inert metal salts like $ZnCl_2$ and $MgCl_2$. Consequently, direct deprotonation reactions were performed with metal complexes provided with internal strong bases such as magnesium and zinc alkyls; however, even in these cases only the neutral radical species $\mathbf{L}^{S\cdot}$ is observed. These unsuccessful metalation reactions reinforce both the ease of oxidation of the dithienyl anion $\mathbf{KL}^{S}$ and the poor coordinating properties of the endocyclic sulfur donor, in line with our previous studies.

Difuran $\mathbf{HL}^{O}$. Replacing the thiophene heterocycles with furan causes a dramatic change in stability, and thus reactivity, of the anionic species. While the reaction between the colorless precursor $\mathbf{HL}^{O}$ and KH in THF results in a color change to dark brown, the ^{1}H NMR spectrum of the reaction mixture is silent and paramagnetic according to qualitative Evans' method measurements; a similarly silent ^{1}H NMR spectrum is seen for the reaction between $\mathbf{HL}^{O}$ and $KN(SiMe_3)_2$. As such, the tendency of the expected anion $\mathbf{KL}^{O}$ to oxidize spontaneously to the radical $\mathbf{L}^{O\cdot}$ is more pronounced than for $\mathbf{KL}^{S}$, and the anionic species $\mathbf{KL}^{O}$ is not even observed. The radical nature of $\mathbf{L}^{O\cdot}$ is corroborated by its EPR spectrum, which is consistent with an organic radical with g_{iso} = 2.0043, albeit with unresolved hyperfine structure (Figure 4). In a previous report, $\mathbf{L}^{O\cdot}$ was prepared but not isolated, either by oxidation of $\mathbf{HL}^{O}$ to form the difurylmethene cation, followed by single-electron reduction by Zn mirror, or by a deprotonation/oxidation protocol similar to that used here.[24] While EPR data were provided for the difuryl complexes in which the *meso*-substituent is either methylfuryl, ethylfuryl, C_6H_4(OH-4), $C_6H_4(^tBu\text{-}3)_2$(OH-4), or C_6H_4(OMe-3) and showed extensive hyperfine structure to the ^{1}H nuclei, no data were provided for $\mathbf{L}^{O\cdot}$. In our case, we were unable to isolate $\mathbf{L}^{O\cdot}$ as an analytically pure compound due to nonstoichiometric incorporation of KI and, as such, the purity of $\mathbf{L}^{O\cdot}$ remains uncertain, with the lack of hyperfine structure seen in the EPR spectrum of $\mathbf{L}^{O\cdot}$ likely a consequence of its coordination to KI. However, the APPI-MS of $\mathbf{L}^{O\cdot}$ provides further support for its identity, showing ions at m/z 251 and 252 consistent with the cations $[\mathbf{L}^{O}]^+$ and $[\mathbf{L}^{O}\text{+H}]^+$ formed on ionization of the radical.

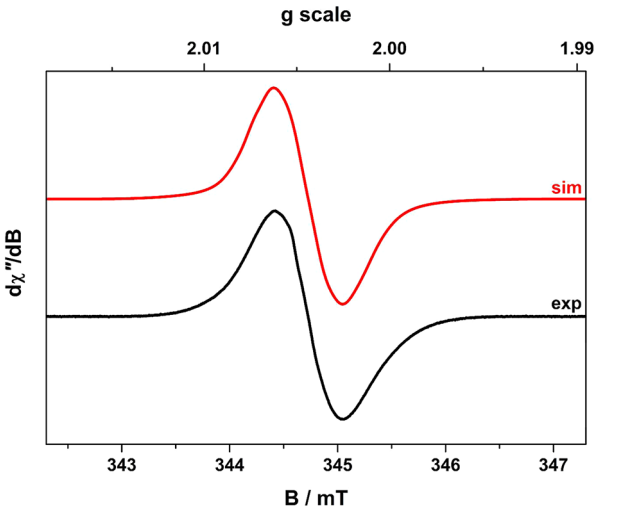

Figure 4. X-band EPR spectrum of radical $\mathbf{L}^{O\cdot}$ in THF at 293 K (experimental conditions: frequency, 9.6709 GHz; power, 10 mW; modulation, 0.1 mT). Experimental data are represented by the black line; simulation is depicted by the red trace composed: g_{iso} = 2.0043; $A_{iso} = 2.2 \times 10^{-4}$ cm^{-1} (2 × ^{1}H); $A_{iso} = 1.6 \times 10^{-4}$ cm^{-1} (2 × ^{1}H); $A_{iso} = 1.5 \times 10^{-4}$ cm^{-1} (2 × ^{1}H); $A_{iso} = 1.1 \times 10^{-4}$ cm^{-1} (1 × ^{1}H).

Iminofuran $\mathbf{HL}^{NO}$. In contrast to the spontaneous oxidation chemistry displayed by the anions $\mathbf{KL}^{S}$ and $\mathbf{KL}^{O}$, the iminofuran $\mathbf{KL}^{NO}$ is straightforwardly isolated as a translucent dark green powder in high yield. Noticeably, $\mathbf{KL}^{NO}$ can be stored under an inert atmosphere in a glovebox for months without any appreciable decomposition. Red crystals of $\mathbf{KL}^{NO}$ suitable for crystallographic analysis were obtained by layering hexanes on a concentrated THF solution. Interestingly, in the solid state, $\mathbf{KL}^{NO}$ exists as a one-dimensional (1D) coordination polymer in which each unit is linked to the next through π-coordination of a furan group to the potassium, with no incorporation of the THF donor solvent (Figure 5).

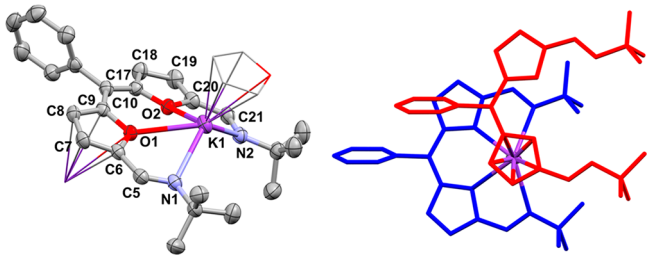

Figure 5. Solid-state structure of the iminofuran anion $\mathbf{KL}^{NO}$. For clarity, all hydrogen atoms and a second molecule in the unit cell are omitted (displacement ellipsoids are drawn at 50% probability). (right) π-Coordination of the furan moiety from the neighboring unit to the K cation. Selected bonds (Å) and angles (deg): K1−O1 2.740(2), K1−O2 2.751(2), K1−N1 2.773(3), K1−N2 2.748(3), N1−C5 1.294(4), N2−C21 1.280(5), O1−C6 1.400(4), O1−C9 1.392(4), C9−C10 1.386 (5), C10−C17 1.418(4), O2−C17 1.386(4), O2−C20 1.396(4); C9−C10−C17 127.4(3), O1−K1−O2 60.31(7), O1−K1−N1 62.56(8), O2−K1−N2 62.40(8), N1−K1−N2 120.15(9).

In the structure, the *meso* carbon C17 is sp^2 hybridized with essentially coplanar iminofuran linkages (torsion angle 8.7°). In contrast to the iminothiophene relative $\mathbf{KL}^{NS}$, which adopts a dimeric structure,[38] the N_2O_2 compartment in $\mathbf{KL}^{NO}$ binds a single potassium cation due to the shorter N1···N2 separation between the imine nitrogen atoms of 4.785(4) Å (compared with 7.357(1) Å in $\mathbf{KL}^{NS}$). Such a feature is also likely responsible for the positioning of the K cation above the N_2O_2 plane (N_2O_2 plane···K1 1.222 Å), although influence by the adjacent π-coordinated furan cannot be excluded (centroid··· K1 3.029 Å).

In a similar manner to the related thiophene anion $\mathbf{KL}^{S}$, reaction between $\mathbf{KL}^{NO}$ and CuI leads to the toluene-soluble, neutral radical $\mathbf{L}^{NO\cdot}$ as a brown/orange solid in good yield, which is isolated as the salt-incorporated adduct KI($\mathbf{L}^{NO\cdot}$). The radical nature of $\mathbf{L}^{NO\cdot}$ is supported by the lack of features in its

DOI: 10.1021/acs.inorgchem.8b00554
Inorg. Chem. XXXX, XXX, XXX−XXX

NMR spectrum and is confirmed by its fluid-solution EPR spectrum, which shows a resonance at g_{iso} = 2.0035, consistent with an organic radical. A complex hyperfine structure arises from the coupling of the unpaired electron with six hydrogen and two nitrogen (^{14}N, I = 1, 99.7% abundant) nuclei from the iminofuryl backbone and three additional hydrogen nuclei from the *meso*-phenyl group (Figure 6).

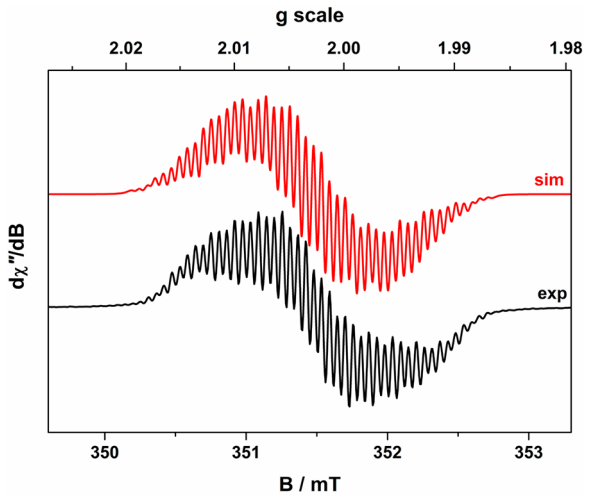

Figure 6. Fluid-solution X-band EPR spectrum of radical $\mathbf{L}^{NO\cdot}$ in THF at 293 K. (Experimental conditions: frequency, 9.8554 GHz; power, 6.3 mW; modulation, 0.01 mT). Experimental data are represented by the black line; simulation is depicted by the red trace composed: g_{iso} = 2.0035; $A_{iso} = 3.54 \times 10^{-4}$ cm^{-1} (2 × ^{1}H); $A_{iso} = 3.22 \times 10^{-4}$ cm^{-1} (2 × ^{1}H); $A_{iso} = 1.60 \times 10^{-4}$ cm^{-1} (3 × ^{1}H); $A_{iso} = 1.57 \times 10^{-4}$ cm^{-1} (2 × ^{1}H); $A_{iso} = 0.53 \times 10^{-4}$ cm^{-1} (2 × ^{14}N).

Electronic Spectroscopy and TD-DFT Analysis. Upon deprotonation of the precursor $\mathbf{HL}^{S}$ to the corresponding potassium salt $\mathbf{KL}^{S}$, two bands at 636 (highest occupied molecular orbital (HOMO)−LUMO) and 465 nm arise in the UV−vis spectrum (Figure 7). Upon oxidation of $\mathbf{KL}^{S}$ into $\mathbf{L}^{S\cdot}$ a weak band at 455 nm is seen, similar in shape to that of $\mathbf{KL}^{S}$, and due to combined α/β singly occupied molecular orbital (SOMO)−LUMO transitions. As in the related thiophene compounds,[38,47] the oxidation of the anion to the radical is accompanied by a hypsochromic shift that is indicative of a larger orbital gap in the radical of 5.50 eV (α-spin) and 5.31 eV (β-spin) against 4.24 eV for the anion. The electronic absorption spectra of the furan-containing compounds are different, in which the HOMO−LUMO transition observed at 284 nm for $\mathbf{HL}^{NO}$ (Figure S11) is modified to multiple bands on deprotonation to $\mathbf{KL}^{NO}$, with the low-energy band at 630 nm associated with the HOMO−LUMO transition (Figure 7). Compared to the thiophene-based diarylmethenes, oxidation of $\mathbf{KL}^{NO}$ to $\mathbf{L}^{NO\cdot}$ does not cause major variations in the electronic spectrum and preserves the slightly red-shifted, four-band motif with the low-energy absorption at 632 nm due to combined α/β SOMO−LUMO transitions. The electronic spectrum of the difuran radical $\mathbf{L}^{O\cdot}$ appears mostly unresolved (Figure S12), with the absorption bands broadened into a large absorption curve and likely caused by the ability of this radical to coordinate nonstoichiometric quantities of KI (see above); precipitation of a colorless solid, presumably KI, is seen during data acquisition.

Electrochemical Studies. Analysis of the cyclic voltammograms (CVs) of the compounds provides additional insight into their electronic properties. The precursor $\mathbf{HL}^{S}$ is electrochemically inert over a potential window spanning

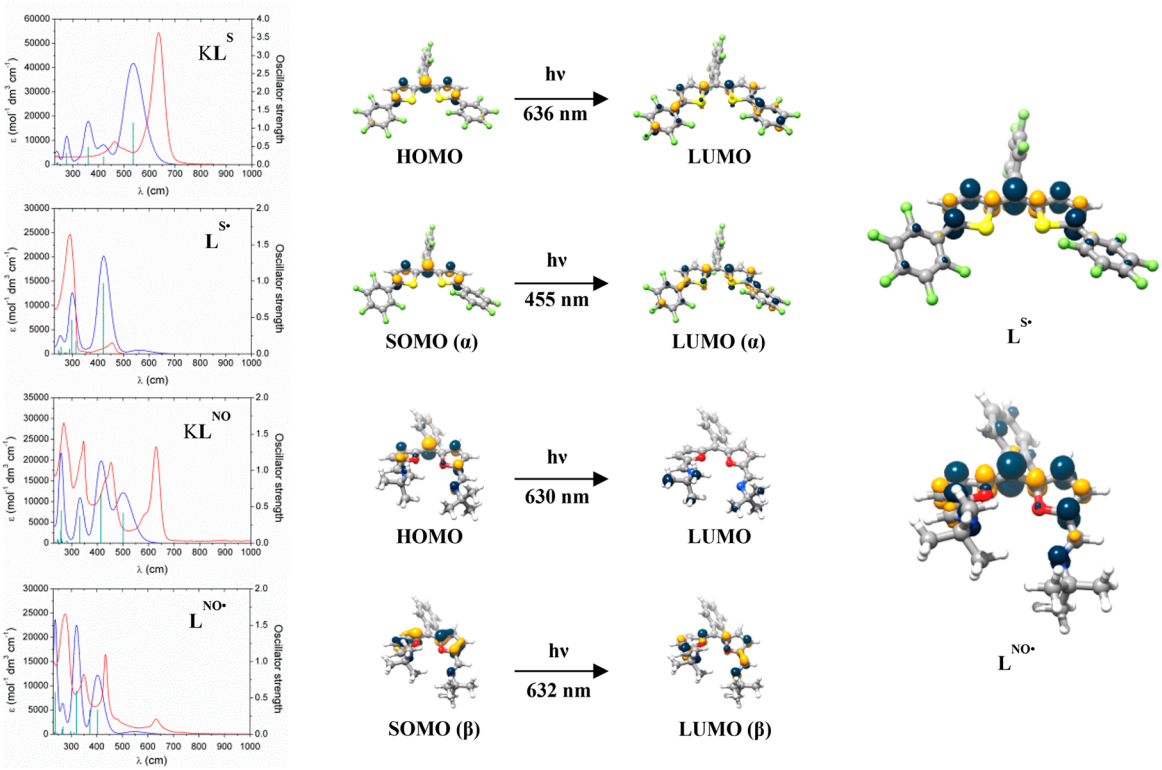

Figure 7. (left) Experimental UV−vis spectra (red trace), TD-DFT calculated spectra (blue trace) and oscillators (green vertical lines). (middle) Principal electronic transitions for each of the four compounds. (right) DFT-calculated spin-density plots for $\mathbf{L}^{S\cdot}$ (top) and $\mathbf{L}^{NO\cdot}$ (bottom).

DOI: 10.1021/acs.inorgchem.8b00554
Inorg. Chem. XXXX, XXX, XXX−XXX

from +1.5 to −2.0 V versus $Fc^{+/0}$. Because of the difficulty in isolating the anion KL^{S}, the electrochemical investigation of $L^{S\cdot}$ is therefore crucial to obtain information on the redox properties of this system. The voltammogram for $L^{S\cdot}$ displays two redox waves, an oxidation at +0.27 V and a reduction and −1.09 V (Figure 8), which are best interpreted as forming the

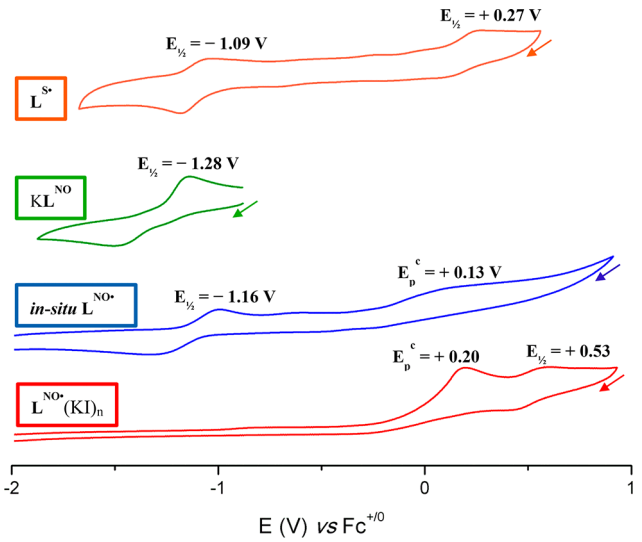

Figure 8. Comparison of CV data for $L^{S\cdot}$ (orange), KL^{NO} (green), $L^{NO\cdot}$ (blue), and $L^{NO\cdot}(KI)_n$ (red); glassy carbon working electrode, platinum gauze counter electrode, silver wire pseudoreference electrode, 100 mV s^{-1}, referenced to $Fc^{+/0}$, 1−5 mM analyte, 0.1 M $[^{n}Bu_4N][PF_6]$ electrolyte in dry CH_2Cl_2 under N_2.

diamagnetic cation L^{S+} upon oxidation, while the reduction event most likely refers to the $L^{S\cdot}/L^{S-}$ couple. No meaningful CV data were acquired for L^{O-} and $L^{O\cdot}$ due to the difficulties encountered in their isolation.

The CV for HL^{NO} comprises three events, namely, an oxidation at −0.11 V and an irreversible oxidation at −0.48 V associated with an irreversible reduction at −1.89 V (Figure S14). On deprotonation to form KL^{NO}, these waves are replaced by a quasi-reversible process at −1.28 V, assigned to the anion-radical redox couple, $KL^{NO}/L^{NO\cdot}$ (Figure 8). Unexpectedly, the CV of isolated $L^{NO\cdot}(KI)_n$ obtained by chemical oxidation of KL^{NO} with CuI does not map on to the wave observed for the anion but instead comprises two oxidations, one irreversible at +0.20 V and one quasi-reversible at +0.53 V, with no trace of the reduction event allied to KL^{NO}. It is therefore evident that the radical formed by chemical oxidation of KL^{NO} by CuI or I_2 has a different composition to that formed by electrochemical oxidation in a noncoordinating electrolyte. As with $L^{O\cdot}(KI)_n$, the unusual electrochemical features of $L^{NO\cdot}(KI)_n$ could derive from the observation by elemental analysis that 1 equiv of KI is incorporated and might therefore alter the redox characteristics of the radical, hampering its reduction to the anion. This is reinforced by the CV of $L^{NO\cdot}$ that is generated in the CV cell by the addition of $Cu^{I}(MeCN)_4BF_4$ to KL^{NO}, which shows the expected $KL^{NO}/L^{NO\cdot}$ redox couple at −1.16 V. The single oxidation seen at 0.13 V is similar to that seen for $L^{NO\cdot}(KI)_n$ at +0.20 V, suggesting that this is a ligand-based oxidation, that is, $L^{+}/L^{NO\cdot}$ and that the second oxidation at +0.53 V relates to the I_2/I^{-} couple. We currently do not fully understand the effect of KI coordination on the redox chemistry of L^{NO} but are exploring this through the synthesis of further examples of complexes of L^{NO} with redox-inert metals.

Compared to the parent iminothiophene compound KL^{NS}, the diarylmethene anions KL^{NO} and KL^{S} investigated here display significantly more facile oxidation chemistry, evident from the highly negative potentials at which the waves related to the formation of the radical species are found. These potentials, at −1.09 and −1.28 V for KL^{S} and KL^{NO}, respectively, are indeed over 1.0 V more negative than that seen for KL^{NS} at −0.12 V and highlight the ease of formation of the radicals. While the oxidation of the anion KL^{NO} is more thermodynamically facile than for KL^{S}, the poorer coordinating ability of the dithienyl donor set to the potassium cation compared to the N_2O_2 donor set likely limits the kinetic stability of KL^{S} and so inhibits its isolation.

CONCLUSIONS

The heterodiarylmethene compounds KL^{S}, KL^{O}, and KL^{NO} have been synthesized and studied by means of spectroscopic, crystallographic, and electrochemical techniques. These conjugated carbanions display a pronounced redox activity and provide stable neutral acyclic radicals upon oxidation under mild conditions. Significantly, the radical $L^{S\cdot}$ was isolated despite a reduction in molecular conjugation compared to $L^{NS\cdot}$ and the incorporation of strongly electron-withdrawing pentafluorophenyl substituents, providing a rare example of a nonmacrocyclic thiophene-based radical.[38,48] Spectroscopic investigation highlighted a shift of the main absorption bands as a consequence of the oxidation of the anion to the corresponding radical and provided evidence of an increased SOMO−LUMO energy gap in the thiophene-derived compound. Electrochemical analysis allowed the identification of the strongly negative potentials at which the oxidation reactions occur, confirming the tendency of these anions to be spontaneously oxidized to the radicals. These results emphasize how the extensive redox activity of diarylmethene carbanions can be controlled by varying the nature of the substituents, donor atom, and the conjugated π-system, and they also emphasize that these variations impact considerably on the coordinating properties of these species; the N_2O_2 donor set of the iminofuran anion allows the isolation and crystallographic characterization of the anion KL^{NO} and promotes KI incorporation in the radical $L^{NO\cdot}$. We are currently exploiting these facets in the development of reagents and catalysts for the reduction of small molecules such as carbon dioxide.

ASSOCIATED CONTENT

Supporting Information

The Supporting Information is available free of charge on the ACS Publications website at DOI: 10.1021/acs.inorgchem.8b00554.

NMR and UV−vis spectra, electrochemical, crystallographic, and computational data (PDF)

Accession Codes

CCDC 1827199 contains the supplementary crystallographic data for this paper. These data can be obtained free of charge via www.ccdc.cam.ac.uk/data_request/cif, or by emailing data_request@ccdc.cam.ac.uk, or by contacting The Cambridge Crystallographic Data Centre, 12 Union Road, Cambridge CB2 1EZ, UK; fax: +44 1223 336033.

DOI: 10.1021/acs.inorgchem.8b00554
Inorg. Chem. XXXX, XXX, XXX−XXX

AUTHOR INFORMATION

Corresponding Author

*E-mail: jason.love@ed.ac.uk.

ORCID

Stephen Sproules: 0000-0003-3587-0375

Jason B. Love: 0000-0002-2956-258X

Author Contributions

The manuscript was written through contributions of all authors. All authors have given approval to the final version of the manuscript.

Funding

EPSRC Centre for Doctoral Training in Critical Resource Catalysis (CRITICAT) EP/L016419/1.

Notes

The authors declare no competing financial interest.

ACKNOWLEDGMENTS

We thank the Univ. of Edinburgh and the EPSRC CRITICAT Centre for Doctoral Training (Ph.D. studentship to M.C.; Grant No. EP/L016419/1).

REFERENCES

(1) Chirik, P. J. Iron- and Cobalt-Catalyzed Alkene Hydrogenation: Catalysis with Both Redox-Active and Strong Field Ligands. *Acc. Chem. Res.* **2015**, *48*, 1687.

(2) Broere, D. L. J.; Plessius, R.; van der Vlugt, J. I. New avenues for ligand-mediated processes - expanding metal reactivity by the use of redox-active catechol, *o*-aminophenol and *o*-phenylenediamine ligands. *Chem. Soc. Rev.* **2015**, *44*, 6886.

(3) Lyons, C. T.; Stack, T. D. P. Recent advances in phenoxyl radical complexes of salen-type ligands as mixed-valent galactose oxidase models. *Coord. Chem. Rev.* **2013**, *257*, 528.

(4) Luca, O. R.; Crabtree, R. H. Redox-active ligands in catalysis. *Chem. Soc. Rev.* **2013**, *42*, 1440.

(5) Lyaskovskyy, V.; de Bruin, B. Redox Non-Innocent Ligands: Versatile New Tools to Control Catalytic Reactions. *ACS Catal.* **2012**, *2*, 270.

(6) Praneeth, V. K. K.; Ringenberg, M. R.; Ward, T. R. Redox-Active Ligands in Catalysis. *Angew. Chem., Int. Ed.* **2012**, *51*, 10228.

(7) Eisenberg, R.; Gray, H. B. Noninnocence in Metal Complexes: A Dithiolene Dawn. *Inorg. Chem.* **2011**, *50*, 9741.

(8) Myers, T. W.; Kazem, N.; Stoll, S.; Britt, R. D.; Shanmugam, M.; Berben, L. A. A Redox Series of Aluminum Complexes: Characterization of Four Oxidation States Including a Ligand Biradical State Stabilized via Exchange Coupling. *J. Am. Chem. Soc.* **2011**, *133*, 8662.

(9) Schweyen, P.; Brandhorst, K.; Wicht, R.; Wolfram, B.; Bröring, M. The Corrole Radical. *Angew. Chem., Int. Ed.* **2015**, *54*, 8213.

(10) Kaim, W. The Shrinking World of Innocent Ligands: Conventionaland Non-Conventional Redox-Active Ligands. *Eur. J. Inorg. Chem.* **2012**, *2012*, 343.

(11) Costentin, C.; Drouet, S.; Robert, M.; Savéant, J. M. A local proton source enhances CO2 electroreduction to CO by a molecular Fe catalyst,. *Science* **2012**, *338*, 90.

(12) Kaim, W.; Schwederski, B. Non-innocent ligands in bioinorganic chemistry—An overview. *Coord. Chem. Rev.* **2010**, *254*, 1580.

(13) McEvoy, J. P.; Brudvig, G. W. Water-splitting chemistry of photosystem II. *Chem. Rev.* **2006**, *106*, 4455.

(14) Römelt, C.; Ye, S.; Bill, E.; Weyhermüller, T.; van Gastel, M.; Neese, F. Electronic Structure and Spin Multiplicity of Iron Tetraphenylporphyrins in Their Reduced States as Determined by a Combination of Resonance Raman Spectroscopy and Quantum Chemistry. *Inorg. Chem.* **2018**, *57*, 2141.

(15) Römelt, C.; Song, J.; Tarrago, M.; Rees, J. A.; van Gastel, M.; Weyhermüller, T.; DeBeer, S.; Bill, E.; Neese, F.; Ye, S. Electronic Structure of a Formal Iron(0) Porphyrin Complex Relevant to CO_2 Reduction. *Inorg. Chem.* **2017**, *56*, 4746.

(16) Chirik, P. J.; Wieghardt, K. Radical Ligands Confer Nobility on Base-Metal Catalysts. *Science* **2010**, *327*, 794.

(17) Nauta, W. T.; Mulder, D. Diarylmethane derivatives VII: Properties of the diphenylmethyl radical. *Recueil Trav. Chim. Pays-Bas* **1939**, *58*, 1070.

(18) Shea, S.; Schepp, N. P.; Keirstead, A. E.; Cozens, F. L. Dynamics of the transient species generated upon photolysis of diarylmethanes within zeolites — Deprotonation and oxidation reactions. *Can. J. Chem.* **2005**, *83*, 1637.

(19) Solodovnikov, S. P.; Kabachnik, M. I. Unpaired electron delocalization in diarylmethane anion-radicals. *Tetrahedron Lett.* **1972**, *13*, 1941.

(20) Young, J. J.; Stevenson, G. R.; Bauld, N. L. Interannular interactions in *p*-substituted diphenylmethane anion radicals. *J. Am. Chem. Soc.* **1972**, *94*, 8790.

(21) Camp, C.; Arnold, J. On the non-innocence of "Nacnacs": ligand-based reactivity in β-diketiminate supported coordination compounds. *Dalton Trans.* **2016**, *45*, 14462.

(22) Chang, M.-C.; Dann, T.; Day, D. P.; Lutz, M.; Wildgoose, G. G.; Otten, E. The Formazanate Ligand as an Electron Reservoir: Bis(Formazanate) Zinc Complexes Isolated in Three Redox States. *Angew. Chem., Int. Ed.* **2014**, *53*, 4118.

(23) Khusniyarov, M. M.; Bill, E.; Weyhermüller, T.; Bothe, E.; Wieghardt, K. Hidden Noninnocence: Theoretical and Experimental Evidence for Redox Activity of a β-Diketiminate(1−) Ligand. *Angew. Chem., Int. Ed.* **2011**, *50*, 1652.

(24) Butin, A. V.; Kul'nevich, V. G.; Abaev, V. T.; Mikhailyuchenko, N. G.; Shpakov, A. V.; Okhlobystin, O. Y.; Zavodnik, V. E.; Lutsenko, A. I. Polyfuryl(aryl)alkanes and their derivatives. 5. Cations and radicals in the polyfuryl(aryl)methane series. *Chem. Heterocycl. Compd.* **1993**, *29*, 274.

(25) Hurmalainen, J.; Mansikkamaki, A.; Morgan, I. S.; Peuronen, A.; Tuononen, H. M. Synthesis and characterisation of p-block complexes of biquinoline at different ligand charge states. *Dalton Trans.* **2017**, *46*, 1377.

(26) Vasko, P.; Kinnunen, V.; O. Moilanen, J.; Roemmele, T. L.; Boere, R. T.; Konu, J.; Tuononen, H. M. Group 13 complexes of dipyridylmethane, a forgotten ligand in coordination chemistry. *Dalton Trans.* **2015**, *44*, 18247.

(27) Moilanen, J.; Borau-Garcia, J.; Roesler, R.; Tuononen, H. M. Paramagnetic aluminium β-diketiminate. *Chem. Commun.* **2012**, *48*, 8949.

(28) Loudet, A.; Burgess, K. BODIPY dyes and their derivatives: syntheses and spectroscopic properties. *Chem. Rev.* **2007**, *107*, 4891.

(29) Koehne, I.; Graw, N.; Teuteberg, T.; Herbst-Irmer, R.; Stalke, D. Introducing NacNac-Like Bis(4,6-isopropylbenzoxazol-2-yl)-methanide in s-Block Metal Coordination. *Inorg. Chem.* **2017**, *56*, 14968.

(30) Dauer, D. R.; Flügge, M.; Herbst-Irmer, R.; Stalke, D. Group 13 metal complexes containing the bis-(4-methylbenzoxazol-2-yl)-methanide ligand. *Dalton Trans.* **2016**, *45*, 6149.

(31) Lecarme, L.; Chiang, L.; Moutet, J.; Leconte, N.; Philouze, C.; Jarjayes, O.; Storr, T.; Thomas, F. The structure of a one-electron oxidized Mn(III)-bis(phenolate)dipyrrin radical complex and oxidation catalysis control via ligand-centered redox activity. *Dalton Trans.* **2016**, *45*, 16325.

(32) Yamamura, M.; Takizawa, H.; Gobo, Y.; Nabeshima, T. Stable neutral radicals of planar N2O2-type dipyrrin platinum complexes: hybrid radicals of the delocalized organic [small pi]-orbital and platinum d-orbital. *Dalton Trans.* **2016**, *45*, 6834.

(33) Dauer, D. R.; Stalke, D. Heterocyclic substituted methanides as promising alternatives to the ubiquitous nacnac ligand. *Dalton Trans.* **2014**, *43*, 14432.

(34) Kochem, A.; Chiang, L.; Baptiste, B.; Philouze, C.; Leconte, N.; Jarjayes, O.; Storr, T.; Thomas, F. Ligand-Centered Redox Activity in Cobalt(II) and Nickel(II) Bis(phenolate)−Dipyrrin Complexes. *Chem. - Eur. J.* **2012**, *18*, 14590.

DOI: 10.1021/acs.inorgchem.8b00554
Inorg. Chem. XXXX, XXX, XXX−XXX

(35) Wijesinghe, C. A.; El-Khouly, M. E.; Subbaiyan, N. K.; Supur, M.; Zandler, M. E.; Ohkubo, K.; Fukuzumi, S.; D'Souza, F. Photochemical Charge Separation in Closely Positioned Donor−Boron Dipyrrin−Fullerene Triads. *Chem. - Eur. J.* **2011**, *17*, 3147.
(36) Pankhurst, J. R.; Cadenbach, T.; Betz, D.; Finn, C.; Love, J. B. Towards dipyrrins: oxidation and metalation of acyclic and macrocyclic Schiff-base dipyrromethanes. *Dalton Trans.* **2015**, *44*, 2066.
(37) Pankhurst, J. R.; Bell, N. L.; Zegke, M.; Platts, L. N.; Lamfsus, C. A.; Maron, L.; Natrajan, L. S.; Sproules, S.; Arnold, P. L.; Love, J. B. Inner-sphere vs. outer-sphere reduction of uranyl supported by a redox-active, donor-expanded dipyrrin. *Chem. Sci.* **2017**, *8*, 108.
(38) Curcio, M.; Pankhurst, J. R.; Sproules, S.; Mignard, D.; Love, J. B. Triggering Redox Activity in a Thiophene Compound: Radical Stabilization and Coordination Chemistry. *Angew. Chem., Int. Ed.* **2017**, *56*, 7939.
(39) Sheldrick, G. M. SHELXT − Integrated space-group and crystal-structure determination. *Acta Crystallogr., Sect. A: Found. Adv.* **2015**, *71*, 3.
(40) Sheldrick, G. Crystal structure refinement with SHELXL. *Acta Crystallogr., Sect. C: Struct. Chem.* **2015**, *71*, 3.
(41) Dolomanov, O. V.; Bourhis, L. J.; Gildea, R. J.; Howard, J. A. K.; Puschmann, H. OLEX2: a complete structure solution, refinement and analysis program. *J. Appl. Crystallogr.* **2009**, *42*, 339.
(42) Frisch, M. J.; Trucks, G. W.; Schlegel, H. B.; Scuseria, G. E.; Robb, M. A.; Cheeseman, J. R.; Scalmani, G.; Barone, V.; Mennucci, B.; Petersson, G. A.; Nakatsuji, H.; Caricato, M.; Li, X.; Hratchian, H. P.; Izmaylov, A. F.; Bloino, J.; Zheng, G.; Sonnenberg, J. L.; Hada, M.; Ehara, M.; Toyota, K.; Fukuda, R.; Hasegawa, J.; Ishida, M.; Nakajima, T.; Honda, Y.; Kitao, O.; Nakai, H.; Vreven, T.; Montgomery, J. A., Jr.; Peralta, J. E.; Ogliaro, F.; Bearpark, M.; Heyd, J. J.; Brothers, E.; Kudin, K. N.; Staroverov, V. N.; Kobayashi, R.; Normand, J.; Raghavachari, K.; Rendell, A.; Burant, J. C.; Iyengar, S. S.; Tomasi, J.; Cossi, M.; Rega, N.; Millam, J. M.; Klene, M.; Knox, J. E.; Cross, J. B.; Bakken, V.; Adamo, C.; Jaramillo, J.; Gomperts, R.; Stratmann, R. E.; Yazyev, O.; Austin, A. J.; Cammi, R.; Pomelli, C.; Ochterski, J. W.; Martin, R. L.; Morokuma, K.; Zakrzewski, V. G.; Voth, G. A.; Salvador, P.; Dannenberg, J. J.; Dapprich, S.; Daniels, A. D.; Farkas, Ö.; Foresman, J. B.; Ortiz, J. V.; Cioslowski, J.; Fox, D. J. *Gaussian 09;* Gaussian Inc.: Wallingford, CT, 2009.
(43) Pettersen, E. F.; Goddard, T. D.; Huang, C. C.; Couch, G. S.; Greenblatt, D. M.; Meng, E. C.; Ferrin, E. T. UCSF Chimera - a visualization system for exploratory research and analysis. *J. Comput. Chem.* **2004**, *25*, 1605.
(44) Do, H. Q.; Daugulis, O. Copper-catalyzed arylation and alkenylation of polyfluoroarene C-H bonds. *J. Am. Chem. Soc.* **2008**, *130*, 1128.
(45) Singh, K.; Virk, T. S.; Zhang, J.; Xu, W.; Zhu, D. Oxygen bridged neutral annulenes: a novel class of materials for organic field-effect transistors. *Chem. Commun.* **2012**, *48*, 121.
(46) Genovese, S.; Epifano, F.; Pelucchini, C.; Curini, M. Preparation of Triaryl- and Triheteroarylmethanes under Ytterbium Triflate Catalysis and Solvent-Free Conditions. *Eur. J. Org. Chem.* **2009**, *2009*, 1132.
(47) Gopalakrishna, T. Y.; Reddy, J. S.; Anand, V. G. An Amphoteric Switch to Aromatic and Antiaromatic States of a Neutral Air-Stable 25π Radical. *Angew. Chem., Int. Ed.* **2014**, *53*, 10984.
(48) Tabakovic, I.; Maki, T.; Miller, L. L.; Yu, Y. Persistent thiophene cation radicals. *Chem. Commun.* **1996**, 1911.

DOI: 10.1021/acs.inorgchem.8b00554
Inorg. Chem. XXXX, XXX, XXX−XXX